Aureusidin Synthase: A Polyphenol Oxidase Homolog Responsible for Flower Coloration

T. Nakayama,[1]* K. Yonekura-Sakakibara,[2]* T. Sato,[1] S. Kikuchi,[1] Y. Fukui,[2] M. Fukuchi-Mizutani,[2] T. Ueda,[3] M. Nakao,[2] Y. Tanaka,[2] T. Kusumi,[2] T. Nishino[1]

Aurones are plant flavonoids that provide yellow color to the flowers of some popular ornamental plants, such as snapdragon and cosmos. In this study, we have identified an enzyme responsible for the synthesis of aurone from chalcones in the yellow snapdragon flower. The enzyme (aureusidin synthase) is a 39-kilodalton, copper-containing glycoprotein catalyzing the hydroxylation and/or oxidative cyclization of the precursor chalcones, 2′,4′,6′,4-tetrahydroxychalcone and 2′,4′,6′,3,4-pentahydroxychalcone. The complementary DNA encoding aureusidin synthase is expressed in the petals of aurone-containing varieties. DNA sequence analysis revealed that aureusidin synthase belongs to the plant polyphenol oxidase family, providing an unequivocal example of the function of the polyphenol oxidase homolog in plants, i.e., flower coloration.

Most floral colors present in nature arise from flavonoids (*1*). Genetic and biochemical knowledge of flavonoid biosynthesis in plants has provided a basis for controlling floral color through genetic engineering approaches (*2*). Aurones (Fig. 1A, **1**) (*3*), a class of plant flavonoids, confer bright yellow color to flowers such as cosmos, coreopsis, and snapdragon (*Antirrhinum majus*) (Fig. 1B). Although the aurone biosynthetic gene(s) is an attractive tool to engineer yellow flowers, the biochemical and genetic details of aurone biosynthesis have remained unclear (*4*). One mechanism proposed for aurone biosynthesis in plants (soy seedling) is a two-step pathway, in which an H_2O_2-dependent peroxidase-catalyzed oxidation of chalcones (Fig. 1A, **2**) yields a 2-(α-hydroxybenzyl)coumaranone derivative, a hydrated form of aurone, which is then dehydrated (Fig. 1C, arrows a and b) (*5*). In this study, we establish that aurone biosynthesis is catalyzed by a homolog of plant polyphenol oxidase (PPO). PPOs ubiquitously occur in higher plants and are responsible for the browning of plant tissues exposed to air. However, the physiological function of PPO in plants remains to be established (*6*). This report demonstrates the participation of a PPO homolog in flower coloration.

The yellow coloration of snapdragon flowers is mainly provided by the glucosides of aurones (aureusidin and bracteatin). Aureusidin can be produced from either 2′,4′,6′,4-tetrahydroxychalcone (THC) or 2′,4′,6′,3,4-pentahydroxychalcone (PHC), whereas bracteatin arises from PHC (*7*) (Fig. 1C, arrows e, f, and g). A single enzyme, which should not be a peroxidase, catalyzes dual chemical transformations, i.e., hydroxylation and oxidative cyclization (2′, α-dehydrogenation), of THC and PHC into aureusidin and bracteatin, respectively (*7*). There-

[1]Department of Biomolecular Engineering, Graduate School of Engineering, Tohoku University, Aoba-yama 07, Sendai 980-8579, Japan. [2]Institute for Fundamental Research, Suntory Ltd., Wakayamadai 1-1-1, Shimamoto-cho, Mishima-gun, Osaka 618-8503, Japan. [3]Kobe Gakuin University, Kobe 651-2180, Japan.

*To whom correspondence should be addressed. E-mail: nakayama@seika.che.tohoku.ac.jp; yskeiko@postman.riken.go.jp

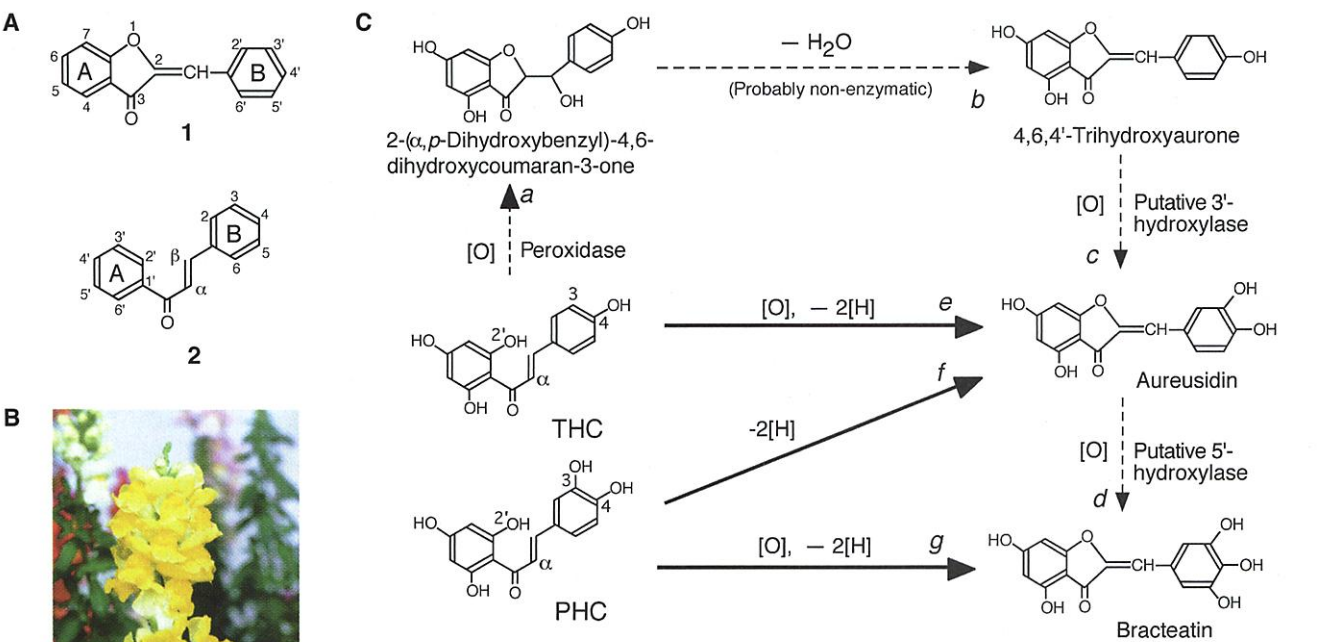

Fig. 1. (**A**) General structures of aurones, **1**, and chalcones, **2**. The positional numbering in the aurones and chalcones is different. A and B shown in the aromatic rings indicate A- and B-rings in the flavonoid structures, respectively. (**B**) Photograph of yellow snapdragon flowers. (**C**) Possible pathways for aurone biosynthesis from chalcones in the snapdragon flowers. Dotted arrows indicate the putative pathway for aurone biosynthesis according to Rathmell *et al.* (*5*). Thick arrows indicate the pathway for aurone biosynthesis identified in this study.

fore, we attempted to purify the enzyme responsible for aurone biosynthesis, which we call aureusidin synthase, from crude extracts of yellow snapdragon flowers.

To purify a sufficient amount of the enzyme, we used 32 kg of snapdragon buds (*8*) as starting material. Moreover, the addition of THC to the buffers used during purification somewhat stabilized enzyme activity. Finally, the enzyme (90 μg) was purified 107-fold to homogeneity by a combination of nine purification steps in an activity yield of 1.4% (Fig. 2) (*8*). The mean value of the final specific activities under the standard assay conditions with THC as a substrate was 578 units mg^{-1} (*9*). However, the specific activity of the enzyme and the actual degree of purification might have been considerably higher, given the instability of this enzyme during the purification. The relative molecular mass (M_r) of the purified aureusidin synthase was estimated to be 40 kD by gel permeation fast protein liquid chromatography on a Superdex 200HR column. The subunit M_r of the enzyme was estimated to be 39 kD by SDS–polyacrylamide gel electrophoresis (SDS-PAGE) (Fig. 2). These results show that the enzyme was monomeric. The aureusidin synthase band in the SDS-PAGE gels was positive to sugar staining (*10*). In addition, the aureusidin synthase was adsorbed on a ConA Sepharose column and was specifically eluted with methyl α-glucoside, indicating that the enzyme is a glycoprotein.

We then determined the amino acid sequences of peptide fragments obtained by lysyl-endopeptidase digestion of the purified synthase essentially as described (*11*). The sequences coincided with the deduced amino acid sequences of a clone that was specifically expressed in the aurone-containing petals, as obtained through a subtractive hybridization approach (*12*). Using this clone as a probe, we isolated a cDNA (termed *AmAS1*) that encodes the precursor of aureusidin synthase from a petal cDNA library of *Antirrhinum majus* (cv. Yellow Butterfly) that had been prepared as described previously (*11*). It contained an open reading frame of 1686 base pairs encoding 562 amino acids. The deduced amino acid sequence showed high similarity to plant PPOs such as those from apple fruit (identity, 51%), grape berry (47%), and potato tuber (39%) (Fig. 3) (*13*, *14*). The predicted M_r (64 kD) of the AmAS1 product was substantially larger than that of the purified aureusidin synthase (39 kD). However, such a difference is consistently explained in terms of the proposed biogenesis of known plant PPOs; plant PPOs are generally synthesized as an ~65-kD precursor protein (*15*), which is subsequently processed into a mature PPO of ~40 kD after removal of a 10-kD NH_2-terminal peptide containing transit sequences (*15*) and a 15-kD COOH-terminal peptide of unknown function (*16*).

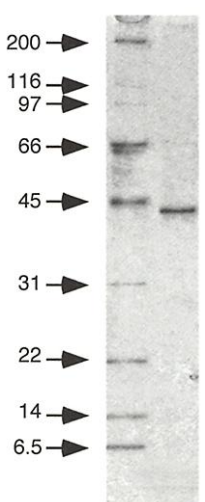

Fig. 2. SDS-PAGE of purified aureusidin synthase. The purified enzyme (right lane) (*8*) was simultaneously subjected to electrophoresis with standard proteins (left lane). Molecular sizes (in kD) are indicated by arrows.

```
AmAS1  M--FKNP--- -NIRYHKLSS ---KSND--- --NDQESSHR C---KHILLF I---I---TL   37
Grape  MASL-PWSLT TSTAIANTTN ISAFPPSPLF QRASHVPVAR NRSRRFAPSK VSCNSANGDP  59
Potato MASVCNSSST -TTTLKTPFI SSNTSLGST- --PKPSQLFL HGKRNKT-FK VSCKVSNSGD  55
                                                   I

AmAS1  F--------- ---------- -LL-IVGLYI ANSLAYAR-F ASTSTGPIAA PDVTKCGQP-  74
Grape  NSDSTSDVRE TSSGKIDRRN VLLGIGGLYG AAGGLGATKP LAF-GAPIQA PDISKCGT-A 117
Potato QN------QN IETNSVDRRN VLLGLGGLYG VA-NAIPLAA SA---TPIPS PDLKTCGRAT 105
                           II

AmAS1  DLPPGTAP-I NCCPPIPAKI IDFELPPPS- ---TTMRVRR AAHLVDDAYI AKFKKAVELM 129
Grape  TVPDGVTP-T NCCPPVTTKI IDFQLPSSG- -SP--MRTRP AAHLVSKEYL AKYKKAIELQ 172
Potato ISDGPLVPY- TCCPPPMPTN FDT-IPYYKF PSMTKLRIRP PAHAVDEEYI AKYNLAISRM 163

AmAS1  RALPE-D--D PRSFKQQANV HCAYCAGAYN QAGFTNLKLQ IHRSWLFFPF HRYYIYFFER 186
Grape  KALPD-D--D PRSFKQQANV HCTYCQGAYD QVGYTDLELQ VHASWLFLPF HRYYLYFNER 229
Potato KDLDKTDPLN PLGFKQQANI HCAYCNGAY- IIG--GKELQ VHNSWLFFPF HRWYLYFYER 220

AmAS1  ILGKLINDTT FALPFWNYDS PGGMTIPSMF IDTNSSLYDS LRDSNHQPPT IVDLNYAFSD 246
Grape  ILAKLIDDPT FALPYWAWDN PDGMYMPTIY ASSPSSLYDE KRNAKHLPPT VIDLDY--DG 287
Potato ILGKLIDDPT FALPYWNWDH PKGMRLPPMF DREGTSIYDE RRNQQVRNGT VMDLGS--FG 278

AmAS1  SDNTTTPEEQ MIINLKIVYR QMVSSAKTPQ LFFGRPYRRG DQEFPGVGSI ELVPHGMIHL 306
Grape  TEPTIPDDEL KTDNLAIMYK QIVSGATTPK LFLGYPYRAG DAIDPGAGTL EHAPHNIVHK 347
Potato DKVQTTQLQL MSNNLTLMYR QMVTNAPCPL LFFGAPYVLG NNVE-APGTI ENIPHIPVHI 337

AmAS1  WTGS------ ENTPY--GEN MGAFYSTARD PIFFAHHSNV DRMWSIWKTL GGPRRTDLTD 358
Grape  WTGL-----A DKPS----ED MGNFYTAGRD PIFFGHHANV DRMWNIWKTI GGKNRKDFTD 398
Potato WAGTVRGSTF PNGDTSYGED MGNFYSAGLD PVFYCHHGNV DRMWNEWKAI GGKRR-DLSE 396

AmAS1  PDFLDASFVF YDENAEMVRV KVRDCLDEKK LGYVYQDVEI PWLNTRPTPK VSPS------ 412
Grape  TDWLDATFVF YDENKQLVKV KVSDCVDTSK LRYQYQDIPI PWL-----PK NTKAKAKTTT 453
Potato KDWLNSEFFF YDENKKPYRV KVRDCLDAKK MGYDYAPMPT PWRNFKPKTK ASVG------ 450

AmAS1  -----LLKK- -FHRTNTANP RQVFPAILDR VLKVIVTRPK KTRSRKEKDE LEEILVIEGI 465
Grape  KSSKSGVAKA AELPKTTISS IGDFPKALNS VIRVEVPRPK KSRSKKEKED EEEVLLIKGI 513
Potato -----KVNT- --TTLPPVNK VFPLTK-MDK AISFSINRPA SSRTQQEKNE QEEMLTFDNI 501

AmAS1  ELERDHGHVK FDVYINADED DLAVISPENA EFAGSFVSLW HKP-IKGKR- TKTQLLTLSI 523
Grape  ELDREN-FVK FDVYINDEDY --SVSRPKNS EFAGSFVNVP HKH-MKEM-- KTKTNLRFAI 567
Potato KYDNRG-YIR FDVFLNVDNN -VNANELDKA EFAGSYTSLP HVHRVGENDH TATVTFQLAI 559

AmAS1  CDILEDLDAD EDDYVLVTLV PRNAGDAIKI HNVKIELDG                        562
Grape  NELLEDLGAE DDESVIVTIV PRAGGDDVTI GGIEIEFVSD                        607
Potato TELLEDIGLE DEETIAVTLV PKKGGEGISI ENVEIKLLDC                        599
```

Fig. 3. Alignment of the deduced amino acid sequence of AmAS1 protein with those of plant PPOs. Amino acid residues identical to that of AmAS1 are shown in red. The dashed underline below the AmAS1 sequence indicates the identification of purified peptides derived from the purified aureusidin synthase. The histidine ligands for the active-site binuclear Cu center, identified in potato PPO by x-ray crystallography (*17*), are shown with black circles. Putative Cu-binding domains (A and B) of AmAS1 are underlined (shown as a and b, respectively). The NH_2-terminal processing sites identified in the PPO sequences of grape and potato and the COOH-terminal processing site identified in that of grape are indicated by vertical lines in the sequence. Sequences of known PPOs representing the "n region" and the "thylakoid transfer domain" are boxed and indicated by I and II, respectively. The nucleotide sequence of AmAS1 has been submitted to the DNA Data Bank of Japan under the accession number AB044884. Abbreviations for the amino acid residues are as follows: A, Ala; C, Cys; D, Asp; E, Glu; F, Phe; G, Gly; H, His; I, Ile; K, Lys; L, Leu; M, Met; N, Asn; P, Pro; Q, Gln; R, Arg; S, Ser; T, Thr; V, Val; W, Trp; and Y, Tyr.

The processing sites in the sequence of the AmAS1 protein remain to be determined because the NH_2-terminus of the purified aureusidin synthase was blocked. The deduced amino acid sequence of the AmAS1 protein contained two putative Cu-binding domains that are conserved in those sequences of the plant PPOs that are binuclear Cu enzymes (*17*). Atomic absorption spectrophotometric analysis of the purified aureusidin synthase allowed us to confirm that it was indeed a binuclear Cu enzyme (*18*).

In accordance with previous observations with crude extracts (*7*), the purified aureusidin synthase could catalyze the 3-hydroxylation and oxidative cyclization of THC to yield aureusidin as a single product, as follows, with an optimum pH of 5.4:

$$\text{THC} + O_2 \rightarrow \text{aureusidin} + H_2O$$

The rate of aureusidin formation from THC was greatly enhanced by H_2O_2, which should act as an enzyme activator. This observation is consistent with the nature of PPO catalysis, where the monophenol monooxygenase activity of PPO is activated by H_2O_2 (*19*). PHC served as a much better substrate than THC (relative activity, 2210%) for the purified aureusidin synthase to produce aureusidin and bracteatin in a molar ratio of 6:1 in the absence of H_2O_2 (*7*). H_2O_2 instead inhibited the reaction with PHC. The formation of aureusidin from PHC was also accompanied by oxygen uptake and proceeded with the following stoichiometry and a broad pH optimum around 5.0 to 7.0:

$$\text{PHC} + \tfrac{1}{2}O_2 \rightarrow \text{aureusidin} + H_2O$$

The 4′-glucosides of THC and PHC were also good substrates (relative activities, 220% and 2496%, respectively). These results prove that the formations of aureusidin and bracteatin from chalcones are single enzymatic processes catalyzed by the same enzyme (Fig. 1C).

The present identification of aureusidin synthase as a homolog of PPO prompted us to examine whether the PPOs generally show aureusidin synthase activity. When the *Neurospora crassa* tyrosinase, a binuclear Cu PPO distantly related to plant PPOs, was reacted with THC (*20*), it also yielded aureusidin as a single product (specific activity, 59 U/mg), establishing the ability of PPO to catalyze aurone synthesis from chalcones. However, aureusidin synthase showed virtually no 3′,4′-dehydrogenation activity toward aureusidin.

The deduced NH_2-terminal amino acid sequence of AmAS1, as well as the properties of aureusidin synthase elucidated in this study, provides important information for insights into the subcellular localization of enzyme. Plant PPOs are localized in plastids (chloroplasts) (*6*); the NH_2-terminal amino acid sequences of the plant PPOs have features that are common to transit peptides known to be targeted to the internal lumen of thylakoid membranes in plastids (*15*) (Fig. 3). However, the localization of aureusidin synthase in plastids is less likely because the deduced NH_2-terminal sequence of the AmAS1 protein does not share such features (*21*). Moreover, glycoproteins are not found localized in plastids. More likely, the enzyme occurs in vacuoles, because 4′-glucosides of THC and PHC, which are very good substrates for the enzyme even without added H_2O_2, are found in vacuoles, and the enzyme activity shows optimum pH's at the pH typical of vacuoles.

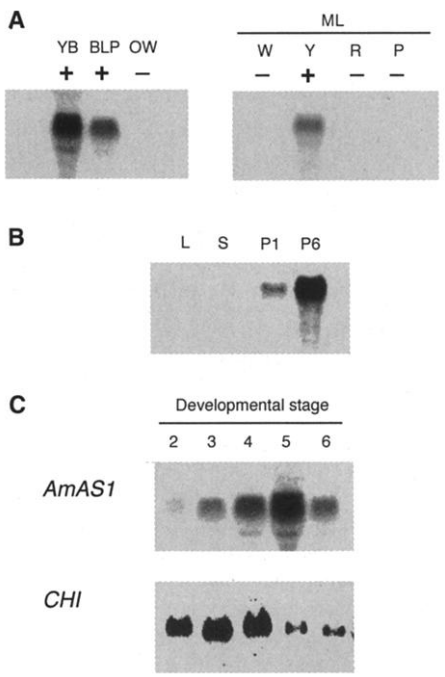

Fig. 4. Northern blot analysis of *AmAS1* gene in snapdragon plants. Ten (A and C) and 20 μg (B) of total RNA were used for each analysis (*11*). (**A**) The expression of *AmAS1* in petals (at stage 5) of different floral color was analyzed. Total RNA was prepared from petals of the following varieties: YB, Yellow Butterfly; BLP, Butterfly Light Pink; OW, Oakland White; ML, Maryland (W, white; Y, yellow; R, red; P, pink). Plus and minus signs indicate the accumulation and absence, respectively, of aurones in the petals (*7*). (**B**) Spatial expression of the *AmAS1* gene in snapdragon plants with yellow flowers. L, 3- to 4-cm-long leaves; S, stems; P1, petals at stage 1; and P6, petals at stage 6. (**C**) The expressions of the *AmAS1* (upper) and the chalcone isomerase genes (*CHI*, lower) in the petals at five different stages of flower development (*7*). To analyze the expressions of *CHI* gene, we amplified partial *CHI* cDNAs by polymerase chain reaction on the basis of the submitted sequence of snapdragon *CHI* cDNA (GenBank accession number M68326). The amplified fragment was identified by DNA sequencing, ^{32}P-labeled, and used as a probe.

To confirm the role of the *AmAS1* gene in flower coloration, we analyzed the spatial and temporal expressions of the *AmAS1* gene in the snapdragon plants (Fig. 4). Northern blot analysis revealed that *AmAS1* was expressed in the aurone-accumulating petals. More *AmAS1* transcripts were found in the petals of yellow varieties than in the petals of pink varieties, which contain small amounts of aurones; and no transcripts were detectable in the aurone-lacking petals of white, pink, and red varieties (Fig. 4A). No transcript was observed in the stem and leaf (Fig. 4B), both of which have no aureusidin synthase activity (*7*). The expression pattern during the development of yellow flowers was also examined. The transcripts were most abundant at stage 5 of flower development (Fig. 4C). Such temporal expression was consistent with the trend observed for aureusidin synthase activity, which was highest at stages 5 and 6 (*7*). Thus, the expression of the *AmAS1* gene is temporally regulated during flower development, as was the case for the genes responsible for anthocyanin biosynthesis (*2*). These results led us to conclude that aureusidin synthase is a plant PPO homolog responsible for the yellow coloration of snapdragon flowers.

References and Notes

1. R. Brouillard, O. Dangles, in *The Flavonoids: Advances in Research Since 1986* (Chapman & Hall, London, 1993), pp. 565–588.
2. Y. Tanaka, S. Tsuda, T. Kusumi, *Plant Cell Physiol.* **39**, 1119 (1998).
3. E. C. Bate-Smith, T. A. Geissman, *Nature* **167**, 688 (1951).
4. M. Shimokoriyama, S. Hattori, *J. Am. Chem. Soc.* **75**, 2277 (1953).
5. W. G. Rathmell, D. S. Bendall, *Biochem. J.* **127**, 125 (1972).
6. K. C. Vaughn, A. R. Lax, S. O. Duke, *Physiol. Plant.* **72**, 659 (1988).
7. T. Sato *et al.*, *Plant Sci.*, in press.
8. Purification was completed at 0° to 5°C; unless otherwise stated, as follows. Enzyme preparation B (*7*) prepared with buffer A [0.01 M sodium acetate (pH 5.0) containing 1 μM THC] from 32 kg of buds [stages 2 to 5 (*7*)], taken from 16,000 stems of yellow snapdragon plant, was dialyzed against 5 mM potassium phosphate (pH 5.0) containing 1 μM THC and 0.3 mM $CaCl_2$ (buffer B). The enzyme solution was then applied to a column of Gigapite hydroxyapatite (Seikagaku, Tokyo) equilibrated with buffer B. The enzyme activity was eluted with a 5 to 500 mM linear gradient of potassium phosphate (without $CaCl_2$). After concentration by ultrafiltration, the concentrate was applied to a HiLoad16/60 Superdex 75 HR column equilibrated with buffer A, containing 0.15 M NaCl and 0.07% CHAPS, and eluted. The active fractions were combined and dialyzed against buffer A containing 0.07% CHAPS. The enzyme solution was applied to a column of SP-Sepharose FF equilibrated with buffer A containing 0.07% CHAPS. The enzyme was eluted with a linear gradient of NaCl (0.04 to 0.32 M) in the same buffer. The active fractions were combined, dialyzed against buffer B containing 0.07% CHAPS, and rechromatographed on a Gigapite column essentially as described above, except that buffer B contained 0.07% CHAPS. To the active fractions, ammonium sulfate was added to 20% saturation. The resultant enzyme solution was applied to a Phenyl-

Sepharose HR5/5 column and eluted by washing the column with 0.01 M potassium phosphate (pH 5.0) containing 0.1% CHAPS and ammonium sulfate at 20% saturation. Active fractions were immediately dialyzed against 0.01 M potassium phosphate (pH 5.0) containing 0.1% CHAPS. The purified enzyme gave a single protein band as judged by silver staining after SDS-PAGE [U. K. Laemmli, *Nature* **227**, 680 (1970)].

9. Aureusidin synthase activity was assayed by reversed-phase high-performance liquid chromatography as described [Method I in (7)]. One unit of enzyme was defined as the amount that catalyzed the formation of 1 nmol of aureusidin per minute. The specific activity of aureusidin synthase was expressed as units/mg of protein. The rate of oxygen consumption during aureusidin synthase reaction was also monitored with the Hansatech DW1/CB1D oxygen electrode system (Hansatech Instruments, Norfolk, UK) (7).
10. J. T. Clarke, *Ann. N.Y. Acad. Sci.* **121**, 428 (1964).
11. H. Fujiwara *et al.*, *Plant J.* **16**, 421 (1998).
12. K. Yonekura-Sakakibara, unpublished results.
13. References and GenBank accession numbers for PPO sequences are as follows: grape [I. B. Dry, S. P. Robinson, *Plant Mol. Biol.* **26**, 495 (1994); S52629]; and potato [P. W. Thygesen, S. P. Robinson, *Plant Physiol.* **109**, 525 (1995); AAA85122].
14. Supplemental Web material is available at *Science Online* at www.sciencemag.org/feature/data/1053401.shl.
15. R. W. Joy IV, M. Sugiyama, H. Fukuda, A. Komamine, *Plant Physiol.* **107**, 1083 (1995).
16. S. P. Robinson, I. B. Dry, *Plant Physiol.* **99**, 317 (1992).
17. T. Klabunde, C. Eicken, J. C. Sacchettini, B. Krebs, *Nature Struct. Biol.* **5**, 1084 (1998).
18. Purified aureusidin synthase was dialyzed in a polystyrene flask at 4°C for 48 hours against metal-free Milli-Q water. The inner and outer solutions for the dialysis were analyzed for Cu content by atomic absorption spectrometry with a model AA-6700F apparatus (Shimadzu).
19. A. Sanchez-Ferrer, J. N. Rodriguez-Lopez, F. Garcia-Canovas, F. Garcia-Carmona, *Biochim. Biophys. Acta* **1247**, 1 (1995).
20. The *N. crassa* PPO (Sigma) was reacted with THC at its optimum pH (6.5) in the absence of H_2O_2 as described (9).
21. PSORT analyses (http://psort.nibb.ac.jp/) did not predict the localization of aureusidin synthase in the plastids .

22 June 2000; accepted 26 September 2000

Survival for Immunity: The Price of Immune System Activation for Bumblebee Workers

Yannick Moret* and Paul Schmid-Hempel

Parasites do not always harm their hosts because the immune system keeps an infection at bay. Ironically, the cost of using immune defenses could itself reduce host fitness. This indirect cost of parasitism is often not visible because of compensatory resource intake. Here, workers of the bumblebee, *Bombus terrestris*, were challenged with lipopolysaccharides and micro–latex beads to induce their immune system under starvation (i.e., not allowing compensatory intake). Compared with controls, survival of induced workers was significantly reduced (by 50 to 70%).

Parasitic infections are pervasive, but hosts often show no obvious effects. Alas, this does not mean that parasites impose no fitness costs on their host, because the immune system is often able to keep the infection within bounds. Recent discussions in the field of evolutionary ecology have concentrated on the idea that the evolution of the immune system is traded off against other fitness components (*1*). In addition, the activation and use of the immune system are thought to be costly and therefore cannot be sustained simultaneously with other demanding activities (*2*). With such costs, the main effect of infection is not the direct damage by the parasite itself but the cost imposed when the host immune system is activated. Why, if these costs exist, are they not more often evident? One reason is that hosts may compensate for increased demand by increased resource intake. Costs are thus masked and no outward signs of a parasitic infection are observed, although the host pays a cost to prevent the establishment and spread of the parasite. To date, such fitness costs have only been shown indirectly, for example, by forcing the individual to increase its parental effort and measuring the corresponding decrease in the immune response (*2*).

Here, the survival cost for the activation of the immune system was analyzed when the host was denied compensation for increased demand. In particular, the host's condition was experimentally "frozen" by adopting a starvation protocol at the point when an "infection"—a standardized immunogenic challenge—occurred (*3*). When an individual is starved, any future allocation to defense reduces the resources available for other needs and thus eventually for maintenance and survival. The starvation paradigm also mimics some important ecological conditions, such as the natural occurrence of adverse weather and limited food availability, that are typical for most animal populations.

In this study, workers of the bumblebee, *Bombus terrestris* L., were used as hosts. Bumblebees are primitively eusocial insects inhabiting temperate habitats where weather conditions often vary over short time periods. Foraging activity is often interrupted by spells of rain and cold weather, leading to the starvation and demise of the colony if workers fail to collect sufficient amounts of pollen and nectar (*4*). Starved workers cannot survive for long (20 to 30 hours). In field populations, most workers are infected by some parasite but nevertheless show normal behaviors and activities (*5*). Bumblebee workers usually do not reproduce themselves. Hence, worker (inclusive) fitness is determined by their survival, and therefore any cost of immunity that reduces survival also reduces fitness (*6*). As in other insects, immunity in bumblebees is innate and based on both cellular (*7*) and humoral mechanisms (*8*). An immune response starts with the recognition of immunogens released by or present on the surface of parasites entering the host hemocoel. Various pathways of the immune system then become activated (*9*), leading to the destruction of the parasite and its removal by cellular reactions such as phagocytosis or encapsulation.

To measure the survival cost of the immune reaction, we experimentally activated the worker's immune system with two kinds of established immune elicitors. (i) Lipopolysaccharides (LPS; Sigma L-2755), i.e., surface molecules extracted from *Escherichia coli*. This nonpathogenic and nonliving elicitor is specifically recognized by pattern recognition proteins of the invertebrate immune system (*9*). LPS induces several pathways of the immune response (*8*, *10*) that persist over many hours (*11*). LPS is cleared from insect hemolymph by lipophorin, a transport protein that shuffles LPS to the fat body (*11*, *12*). Hence, the clearance of LPS should not involve processes that are responsible for clearing bacteria from the hemolymph such as phagocytosis. (ii) Sterile micro–latex beads (Polysciences; diameter 4.5 μm). These beads are a similar size to bacteria and are cleared from the hemolymph by a combination of processes (*8*, *10*), including phagocytosis. In both cases, the immune system is activated, but the artificial "parasite" is unable to generate any pathogenic effect.

A first experiment tested whether decreased survival might result from a toxic side effect of the immune elicitors, assuming that such effects would also decrease the survival of nonstarved animals. In addition, survival should then correlate with dose (*13*).

Eidgenössische Technische Hochschule (ETH) Zürich, Experimental Ecology, ETH-Zentrum, NW, CH-8092 Zürich, Switzerland.

*To whom correspondence should be addressed. E-mail: moret@eco.umnw.ethz.ch